Landscape Ecol (2009) 24:433–450
DOI 10.1007/s10980-009-9327-y

RESEARCH ARTICLE

Surface metrics: an alternative to patch metrics for the quantification of landscape structure

Kevin McGarigal · Sermin Tagil · Samuel A. Cushman

Received: 9 October 2008 / Accepted: 19 January 2009 / Published online: 1 February 2009

Abstract Modern landscape ecology is based on the patch mosaic paradigm, in which landscapes are conceptualized and analyzed as mosaics of discrete patches. While this model has been widely successful, there are many situations where it is more meaningful to model landscape structure based on continuous rather than discrete spatial heterogeneity. The growing field of surface metrology offers a variety of surface metrics for quantifying landscape gradients, yet these metrics are largely unknown and/or unused by landscape ecologists. In this paper, we describe a suite of surface metrics with potential for landscape ecological application. We assessed the redundancy among metrics and sought to find groups of similarly behaved metrics by examining metric performance across 264 sample landscapes in western Turkey. For comparative purposes and to evaluate the robustness of the observed patterns, we examined 16 different patch mosaic models and 18 different landscape gradient models of landscape structure. Surface metrics were highly redundant, but less so than patch metrics, and consistently aggregated into four cohesive clusters of similarly behaved metrics representing surface roughness, shape of the surface height distribution, and angular and radial surface texture. While the surface roughness metrics have strong analogs among the patch metrics, the other surface components are largely unique to landscape gradients. We contend that the surface properties we identified are nearly universal and have potential to offer new insights into landscape pattern–process relationships.

Keywords Landscape gradient model · Surface patterns · Landscape heterogeneity · Landscape metrics · Landscape pattern

Electronic supplementary material The online version of this article (doi:10.1007/s10980-009-9327-y) contains supplementary material, which is available to authorized users.

K. McGarigal (✉)
Department of Natural Resources Conservation,
University of Massachusetts, Amherst, MA 01003, USA
e-mail: mcgarigalk@nrc.umass.edu

S. Tagil
Department of Geography, Balikesir University,
10100 Balikesir, Turkey

S. A. Cushman
USDA Forest Service, Rocky Mountain Research Station,
Forestry Sciences Laboratory, Missoula, MT 59801, USA

Introduction

Modern landscape ecology is based on the patch mosaic paradigm, in which landscapes are conceptualized and analyzed as mosaics of discrete patches (Forman 1995; Turner et al. 2001). Sometimes the

"patch mosaic" model is referred to as the "patch-corridor-matrix" model after Forman and Godron (1986) and Forman (1995) in order to recognize the different major landscape elements that can be present in a patch mosaic. Any reading of the published landscape ecology literature shows near uniformity in the adoption of this approach. Consequently, our current state of knowledge regarding landscape pattern–process relationships is based almost entirely on a categorical representation of spatial heterogeneity. The patch mosaic model has led to major advances in our understanding of landscape pattern–process relationships (Turner 2005), and has proven extraordinarily robust, being applied successfully to landscapes across the globe. The strength of the patch mosaic model lies in its conceptual simplicity and appeal to human intuition. In addition, the patch mosaic model is consistent with well-developed and widely understood quantitative techniques designed for discrete data (e.g., analysis of variance), and there is ample evidence that it applies very well in landscapes dominated by severe natural or anthropogenic disturbances (e.g., fire dominated landscapes and built landscapes) where sharp discontinuities have been created by disturbance.

Despite the progress made in understanding and managing landscapes based on the patch mosaic model, there are many situations where the patch mosaic model fails or is at best sub-optimal. In particular, the patch mosaic model does not accurately represent continuous spatial heterogeneity (McGarigal and Cushman 2005). Once categorized, patches subsume all internal heterogeneity, which may result in the loss of important ecological information. When applying the patch mosaic model in practice, it is prudent to ask whether the magnitude of information loss is acceptable. We contend that there are many situations when the loss is unacceptable. Most ecological attributes are inherently continuous in their spatial variation (at least at some scales; Wiens 1989), even in human-dominated landscapes. Consider soil properties such as depth, texture and chemistry, and terrain properties such as elevation, slope and aspect. These physical environmental properties typically vary continuously over space despite discontinuities in above-ground land cover that might exist due to natural or anthropogenic disturbances. Even above-ground land cover defined on the basis of vegetation more often than not varies continuously along underlying environmental gradients, except where humans have substantially modified it (Austin and Smith 1989; Austin 1999a, b).

These observations have led several authors to propose alternatives to the patch mosaic model for situations where spatial heterogeneity is continuous rather than discrete. McIntyre and Barrett (1992) introduced the "variegation" model as an alternative to the "island biogeographic" model, in which habitat is viewed as a continuous gradient instead of discrete patches within a homogeneous matrix. Later, Manning et al. (2004) defined the ''continua-umwelt" model as a refinement of the variegation model in which habitat gradients are species-specific and governed by ecological processes in a spatially continuous and potentially complex way. Fischer and Lindenmayer (2006) offered an additional refinement of the continua-umwelt model by suggesting that the landscape be defined on the basis of four specific habitat gradients (food, shelter, space, and climate) that are closely related to ecological processes that affect the distribution of animals. Importantly, these alternative conceptual models are all habitat-centric; that is, they propose a gradient model of "habitat"; they do not provide a general purpose model of landscape structure.

McGarigal and Cushman (2005) introduced the "landscape gradient" model, a general conceptual model of landscape structure based on continuous rather than discrete spatial heterogeneity. In this model, the underlying heterogeneity is viewed as a three-dimensional surface and can represent any ecological attribute(s) of interest. The most common example of a landscape gradient model is a digital elevation surface, but there are many other possibilities. Of course McGarigal and Cushman (2005) were not the first to recognize the need to characterize three-dimensional surfaces for ecological purposes. Geomorphologists, for example, have long sought ways to characterize land surfaces for the purpose of understanding the relationships between landforms and geomorphological processes (e.g., Strahler 1952; Schumm 1956; Melton 1957), and biologists as early as 1983 have sought ways to assess topographic roughness for the purpose of characterizing fish and wildlife habitat (e.g., Beasom 1983; Sanson et al. 1995). To this end, many methods have been developed to quantify surface complexity (e.g., Pike 2000; Wilson and Gallant 2000; Jenness 2004).

However, until recently these methods have focused almost exclusively on characterizing topographic surfaces at the scale of the individual pixel or cell (e.g., Moore et al. 1991; Jenness 2005), or as the basis for mitigating the source of error associated with the planimetric projection of slopes in the calculation of patch metrics (e.g., Dorner et al. 2002; Hoechstetter et al. 2008). Only recently has attention been given to the application of surface metrics for the purpose of quantifying surface heterogeneity at the scale of entire landscapes (McGarigal and Cushman 2005; Hoechstetter et al. 2008).

Largely unknown to landscape ecologists, researchers involved in microscopy and molecular physics have made significant advances in the area of three-dimensional surface analysis, creating the field of surface metrology (Stout et al. 1994; Barbato et al. 1995; Villarrubia 1997; Ramasawmy et al. 2000). Over the past two decades structural and molecular physicists have been developing surface metrics which we believe will be highly applicable to landscape gradients (e.g., Gadelmawla et al. 2002). Until recently, however, there have been no landscape ecological applications of these surface metrics. The purpose of this paper is to describe the use of surface metrics for quantifying landscape patterns. Our specific objectives are to: (1) clarify the relationship between the patch mosaic and gradient models of landscape structure and the metrics used to characterize landscapes under each model; (2) describe a variety of surface metrics with the potential for quantifying the structure of landscape gradients; (3) evaluate the behavior of a large suite of surface metrics across 264 sample landscapes and 18 alternative landscape gradient models of landscape structure; and (4) discuss the challenges to the application of surface pattern metrics in landscape ecological investigations.

Methods

Study area

To evaluate and illustrate the use of surface metrics we delineated a 1,988 km^2 montane landscape in western Turkey. The landscape is located between the towns of Aytinova and Altinoluk on the Gulf of Edremit in the western part of the Marmara Regions between 26°36′–27°21′N latitude and 39°10′–39°46′E longitude (Fig. 1). The terrain is rugged and ranges from sea level to 1,769 m in elevation. Geologic formations are primarily marine sandstones and shales, granite, basaltic volcanic rocks, and related intrusives. Most soils are well drained and have well-developed horizons. Soils on steep slopes tend to be shallow and stony loam-textured, whereas soils on uneven and unstable slopes are deeper and derived from colluviums. The overall climate is maritime Mediterranean, with cold wet winters and hot dry summers. Land cover is highly variable owing to a mixture of land uses. Forest, maquis, and garrigue vegetation is interspersed with settlements and agriculture. Dominant tree species include *Quercus* sp., *Pinus* spp., *Juniperus* sp., *Abies equi-trojani*, *Castanea sativa*, *Populus* sp., *Fagus* sp., *Cedrus libani*, and *Carpinus betulus*. The landscape includes one large protected area, Mount Ida National Park, but otherwise the land cover reflects a long history of human land uses.

Spatial data

To examine the robustness of the relationships being examined we constructed several alternative patch mosaic and gradient models of landscape structure. The purpose of doing this was to ensure that any findings were not idiosyncratic given the many ways one can represent landscape structure.

We created eight different patch mosaics using categorical data obtained from various Turkish General Directorates (Table 1). All of these mosaics represented realistic landscape models as used in forest management plans in the region. Six of the mosaics are land cover maps derived from aerial photographs (1:15,000) and field data. Two of the mosaics (GEO and SOILS) are classifications based on physical substrate. In these latter two cases, we aggregated a rather large number of original classes into a smaller set of classes based on shared physical attributes. In all cases, the original data were in vector format with a minimum polygon size of 3.7 ha. For the landscape pattern analysis, we converted the vector coverages to raster data sets using a cell size of 28.5 m for consistency with the Landsat Enhanced Thematic Mapper (ETM+) data below.

We created nine different gradient models using continuous data obtained from Landsat ETM+ and a Digital Elevation Model (DEM) (Table 2). All of these gradient surfaces represented realistic landscape

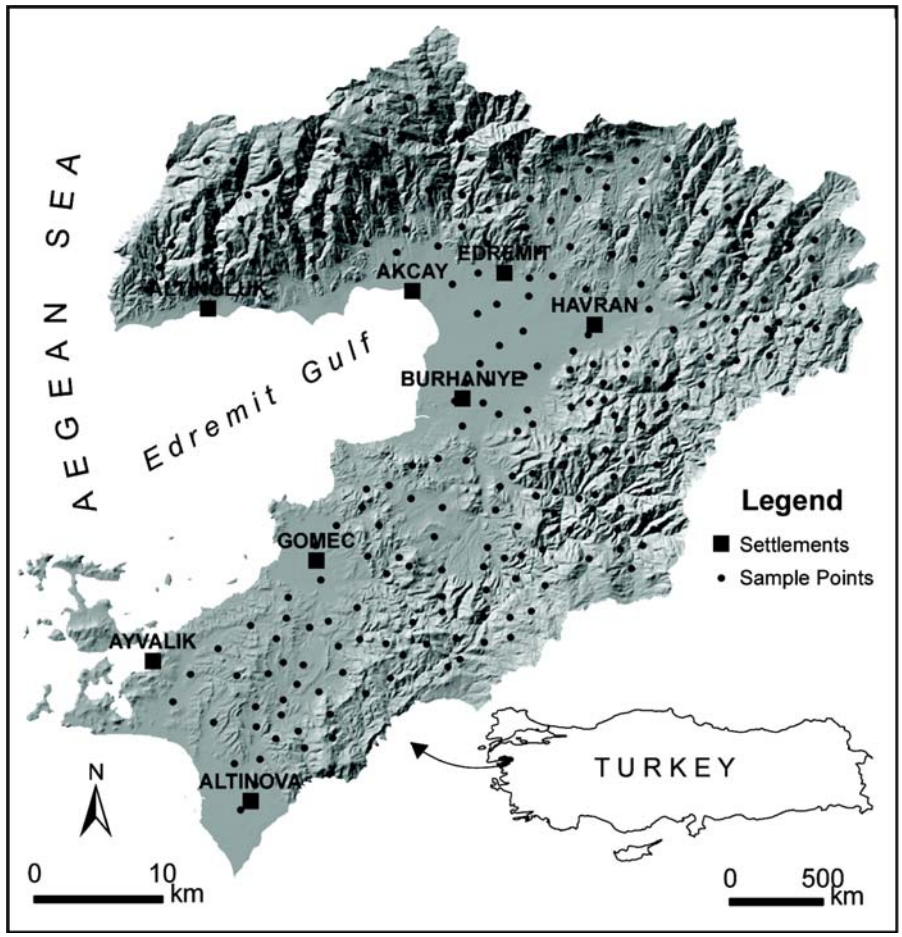

Fig. 1 Study area located in western Turkey. *Solid circles* represent 264 random sample locations

models as used in a wide variety of ecological applications. Five of the gradient models represented various terrain-based indices (i.e., derived from the DEM) hypothesized to be important determinants of the distribution of plants and ecological communities (e.g., Parker and Bendix 1996). Four of the gradient models represented various land cover indices (i.e., the Normalized Difference Vegetation Index (NDVI), and three Tasseled Cap indices) derived from ETM+ imagery acquired in June, 2000. Before deriving these indices, we geometrically corrected the raw ETM+ image based on 50 ground control points taken from 1:25,000 topographic maps; the root mean square error was less than 0.5 pixels.

Sampling design and data analysis

We selected 264 sample locations at random throughout the study area maintaining a minimum distance of 1,000 m between sample points, and between points and the landscape boundary (Fig. 1). At each sample location we clipped each of the 17 spatial data sets (i.e., 8 patch mosaic models and 9 landscape gradient models) using 1000 × 1000 m and 2000 × 2000 m square windows centered on the point. The square-shaped window was required by the software used to compute the surface metrics (see below) and is currently a limitation of available software. The two window sizes selected represented a compromise between maximizing the number of independent samples that could be drawn from the landscape and maintaining a sufficiently large spatial extent to capture the inherent heterogeneity of the landscape. Smaller extents too often resulted in landscapes with no spatial heterogeneity in one or more of the maps and larger landscapes reduced the sample size too much.

For the categorical data (8 patch mosaics × 2 window sizes × 264 sample landscapes), we

Table 1 Patch mosaics created using categorical data obtained from the Turkish General Directory of Forestry (GDF), General Directory of Mineral Research and Exploration (GDMRE), and General Directory of Rural Services (GDRS). All GDF land cover maps were derived from aerial photographs (1:15,000) and field data. Geology and soils maps were from 1:25,000 scaled digital maps from GDMRE and GDRS, respectively

Patch mosaic	Description
Stand type (STND)	Distinguished on the basis of crown closure, stand development stage and tree species. There are 191 classes
Stand development stage (STG)	Based on average diameter at breast height of trees. There are 6 classes: youth and stick (1–7.9 cm), stick and pole (8–19.9 cm), thin (20–35.9 cm), middle (36–51.9 cm), thick (>52 cm), and mixed diameter stands
Crown closure (CLSR)	Percent of the ground covered by tree canopy. There are 4 classes: <10%, 11–40, 41–70, and 70–100%
Site quality (QLTY)	Ordinal scale index of site productivity based on factors such as climate, topography and soil. There are 5 classes: 1, 2, 3, 4, 5 (where 1 is the highest site quality)
Mixture code (MXTR)	Based on the dominant tree species. There are 10 classes: uncovered, *Pinus brutia*, *Pinus nigra*, *Abies* sp., *Cedrus libani*, *Pinus pinea*, *Fagus* sp., *Quercus* sp., mixed coniferous stand, and mixed coniferous–deciduous stand
Landuse and landcover (LULC)	Based on the dominant human land use and the dominant life form of vegetation. There are 8 classes: forest, degraded forest, grassland, agriculture, exposed rock and soil, water, marshland, and settlement
Geology (GEO)	Based on the formation. There are 6 classes: neogene marine formation (e.g., granodiorite), metamorphic rocks (e.g., marble, gneiss, schist, shale), orogenic rocks (e.g., serpantinite), volcanic rocks (e.g., andesite, dacite tuff, basalt), sedimentary rocks (e.g., sandstone, mudstones, limestone), and alluvial deposits
Soils (SOIL)	Based on soil type. There are 10 classes: alluvial soil, colluvial soil, non-calcic brown forest soil, sediment deposited in beach, brown forest soils, rendzina, non-calcic brown soils, hydromorphic alluvial soils, red-brown Mediterranean forest soils, high mountain pasture soils

calculated 28 landscape-level metrics using FRAGSTATS (McGarigal et al. 2002; Table 3). We selected a suite of commonly used metrics with the aim of capturing a broad suite of landscape structure components (Neel et al. 2004; Cushman et al. 2008). All of the metrics were structural metrics except for three metrics based on edge contrast. For each patch mosaic model, we established edge contrast weights for each pairwise combination of classes based on a combination of expert knowledge and quantitative data (e.g., percent canopy closure).

For the continuous data (9 gradient surfaces × 2 window sizes × 264 sample landscapes), we calculated 18 surface metrics using the Scanning Probe Image Processor (SPIP) software. For this study, we selected a suite of surface metrics that measure various aspects of surface texture that have an ecological interpretation (Appendix—Electronic Supplementary Material). All metrics were computed employing a correction for the surface mean. This correction was applied to each of the sample landscapes to remove the differences in the mean absolute height of the surface among sample landscapes and focus the comparison among landscapes on the relative differences in surface roughness. After preliminary analyses, we dropped dominant radial wavelength (*Srw*) from the analysis due to the lack of variation among sample landscapes in some subsets of the data. Thus, the final data set consisted of 17 surface metrics.

To evaluate the degree of redundancy among landscape metrics we used principal components analysis (PCA). Briefly, we conducted a separate PCA for each landscape model, including 16 patch mosaic models (8 mosaics × 2 window sizes) and 18 landscape gradient models (9 surfaces × 2 window sizes). PCA was based on the correlation matrix of the metrics (28 patch metrics or 17 surface metrics) and was deemed appropriate after examining pairwise scatterplots among metrics (McGarigal et al. 2000). To summarize the results of the PCA, we calculated the number of PC's required to account for >95% of the variation in each data set, where each data set was comprised of 264 sample landscapes at one of the two window sizes for a single landscape model (e.g., DEM). We also conducted a Monte Carlo randomization test of significance of the eigenvalues from each model. The Monte Carlo test involved randomly shuffling each column of the data matrix to remove

Table 2 Gradient surfaces created from 28.5-m-resolution Landsat ETM+ and a Digital Elevation Model (DEM) at the same resolution

Gradient surface	Description
Digital elevation model (DEM)	Based on a digital elevation model derived from 10 m-interval contours on 1:25,000 topographic maps
Slope (SLP)	Percent slope derived from the DEM
Topographic wetness (TWI)	Based on Moore et al. (1993); accounts for the propensity of a site to be wet or dry. Positive values tend towards wetter sites; negative values tend towards drier sites
Topographic position index (TPI500)	Based on Jenness (2005) using a 500 m neighborhood. Positive values tend towards ridgetops, negative values tend toward valley bottoms, and zero values tend toward flat areas and mid-slopes
Heat load index (HLI)	Based on McCune and Keon (2002); accounts for potential solar radiation as a function of latitude, aspect and slope. Larger values indicate increased solar radiation
Normalized difference vegetation index (NDVI)	Derived from ETM+ and calculated as the ratio of the difference between near infrared (r NIR) and red (r red) reflectance divided by their sum (ERDAS 1999): (r NIR- r red)/(r NIR+ r red). NDVI values range between −1 and +1, where negative values generally indicate water, 0 indicates no green vegetation, and larger positive values indicate increasing density/biomass of green vegetation, with values typically ranging from 0.05 for sparse vegetative cover to 0.7 for dense vegetative cover (Tucker 1979)
Tasseled cap brightness (TsBR)	Derived from ETM+ and calculated as: brightness = 0.3037(TM1) + 0.2793(TM2) + 0.4743(TM3) + 0.5585(TM4) + 0.5082(TM5) + 0.1863(TM7)
Tasseled cap greenness (TsGR)	Derived from ETM+ and calculated as: greenness = −0.2848(TM1)− 0.2435(TM2) − 0.5436(TM3) + 0.7243(TM4) + 0.0840(TM5) − 0.1800(TM7)
Tasseled cap wetness (TsWET)	Derived from ETM+ and calculated as: wetness = 0.1509(TM1) + 0.1973(TM2) + 0.3279(TM3) + 0.3406(TM4) − 0.7112(TM5) − 0.4572(TM7)

any real correlation structure, computing the eigenvalues for the randomly permuted data matrix, repeating this process 1,000 times, and comparing the original eigenvalue to the random distribution of eigenvalues. This test provides the probability of observing the original eigenvalue if in fact it was derived from a data set without any real correlation structure. Lastly, we constructed a cumulative scree plot of the eigenvalues from each model, which depicts the cumulative percentage of variance explained by an increasing number of principal components (McGarigal et al. 2000).

To identify groups of highly correlated surface metrics for purposes of seeking a parsimonious characterization of surface properties, we used polythetic agglomerative hierarchical cluster analysis (McGarigal et al. 2000). For each of the landscape gradient models, we created a distance matrix representing the pairwise dissimilarities between landscape metrics using the absolute value of their rank-based correlations. Specifically, the "distance" between each pair of metrics was defined as 1-abs(*rho*), where *rho* is the Spearman rank correlation coefficient. In this manner, two metrics had a distance of zero if they were perfectly correlated, either positively or negatively, and a distance of one if they were independent (i.e., *rho* = 0). We used Spearman's rank correlation to allow for nonlinear, but monotonic relationships between landscape metrics. Hierarchical clustering was conducted using Ward's minimum-variance fusion method, given our desire to identify discrete clusters (McGarigal et al. 2000). To summarize the results of the cluster analysis, we produced a scree plot for each model, which depicts the dissimilarity at which clusters fuse together. We also examined the dendrogram from each model to identify which metrics were grouping together and to get a sense of the strength of the cluster solution. To quantify the

Table 3 Patch metrics computed using FRAGSTATS (McGarigal et al. 2002). See FRAGSTATS manual for a detailed description of each metric

Metric
Patch density (*PD*)
Largest patch index (*LPI*)
Edge density (*ED*)
Mean patch area (*AREA_MN*)
Area-weighted mean patch area (*AREA_AM*)
Coefficient of variation in patch area (*AREA_CV*)
Mean patch radius of gyration (*GYRATE_MN*)
Area-weighted mean patch radius of gyration (*GYRATE_AM*)
Coefficient of variation in patch radius of gyration (*GYRATE_CV*)
Mean patch shape index (*SHAPE_MN*)
Area-weighted mean patch shape index (*SHAPE_AM*)
Coefficient of variation in patch shape index (*SHAPE_CV*)
Mean patch contiguity index (*CONTIG_MN*)
Area-weighted mean patch contiguity index (*CONTIG_AM*)
Coefficient of variation in patch contiguity index (*CONTIG_CV*)
Mean Euclidean nearest neighbor distance (*ENN_MN*)
Area-weighted mean Euclidean nearest neighbor distance (*ENN_AM*)
Coefficient of variation in Euclidean nearest neighbor distance (*ENN_CV*)
Contrast-weighted edge density (*CWED*)
Total edge contrast index (*TECI*)
Mean patch edge contrast index (*ECON_MN*)
Area-weighted mean patch edge contrast index (*ECON_AM*)
Coefficient of variation in patch edge contrast index (*ECON_CV*)
Contagion (*CONTAG*)
Patch richness density (*PRD*)
Simpson's diversity index (*SIDI*)
Simpson's evenness index (*SIEI*)
Aggregation index (*AI*)

strength of the clustering structure, we also computed the agglomeration coefficient (AC) for each model. AC ranges from zero to one and approaches one as the strength of the clustering structure increases. A strong clustering structure is one in which within-cluster similarity is very high and among-cluster similarity is very low. Lastly, to examine the integrity of the final clusters, we computed an index of cluster cohesiveness, using a four step approach. First, after examining the scree plots and dendrograms, we determined the final number of clusters to retain. Second, we computed the proportion of models in which each landscape metric co-occurred in the same cluster with each other metric. Third, we assigned each metric to the cluster that it most often fell into across the different landscape models. Finally, we computed the average proportion of co-occurrence among the metrics in each cluster. The resulting cohesiveness index ranges from zero to one and equals one if the cluster members (surface metrics) always co-occur with each other across alternative models of landscape structure.

To aid in the ecological interpretation of the clusters defined above, we created three patch mosaic models each from the DEM and NDVI surfaces by classifying them into 5, 10, and 15 classes (patch types) based on natural breaks. The multiple classifications represented our uncertainty in how thematic resolution would affect the correlation between surface and patch metrics. Importantly, the corresponding gradient surface and patch mosaics represented the same underlying ecological heterogeneity (i.e., variation in elevation or vegetation biomass), but did so in a very different manner. We sought to compare the surface metrics computed from the gradient surface with the patch metrics computed from the corresponding patch mosaics in order to better understand the ecological meaning of the surface metrics given our experience and understanding of patch metrics. To do so, we computed the Spearman rank correlations between each surface metric and each of the patch metrics for the corresponding landscape models (e.g., the DEM surface compared to the DEM patch mosaic based on 5 classes). After preliminary inspection of the results we decided to average the correlations across the three resolutions since the patterns were similar. Thus, we ended up with an average Spearman rank correlation between each surface metric and each patch metric for the DEM models and for the NDVI models.

All statistical analyses were conducted using R (R Development Core Team 2008), including basic functions in the stats library and programs written by the authors.

Results

Both patch and surface metrics exhibited a high degree of redundancy based on PCA. Surface metrics exhibited less redundancy than patch metrics, a

pattern consistent across alternative models of landscape structure. Among the 16 patch mosaic models (8 mosaics × 2 window sizes), it required an average of 6 (range 4–8) principal components to account for more than 95% of the total variance in all 28 patch metrics, with an average of 2.25 (range 2–3) significant components based on the Monte Carlo test. Among the 18 landscape gradient models (9 surfaces × 2 window sizes), it required an average of 8 (range 7–9) principal components to account for more than 95% of the total variance in all 17 surface metrics, with an average of 3.7 (range 3–5) significant components based on the Monte Carlo test. The high level of redundancy among metrics in both sets of models is apparent in the cumulative scree plots (Fig. 2). The pronounced inverted elbow shape to the curves reflects the high degree of redundancy among metrics in both sets of models. The differences between curves reflects the lower redundancy among surface metrics compared to patch metrics, and the narrow range of variation about both the median curves reflects the high degree of consistency in redundancy patterns across alternative landscape models.

Surface metrics consistently aggregated into three or four groups based on hierarchical clustering. The scree plot shows a pronounced "elbow" at three or possibly four clusters, a pattern that was highly consistent across alternative landscape models (Fig. 3). The hierarchical clustering of metrics is better visualized as a dendrogram, as depicted in Fig. 4 for a representative model. This particular dendrogram reveals a strong three-cluster solution, which was ubiquitous across landscape models, and a weaker four-cluster solution, which was nearly universal. The agglomeration coefficient averaged 0.91 (range 0.89–0.92) across landscape models indicating a strong clustering structure. The cohesiveness of the four clusters varied somewhat (Fig. 5). Both the first cluster (comprised of five

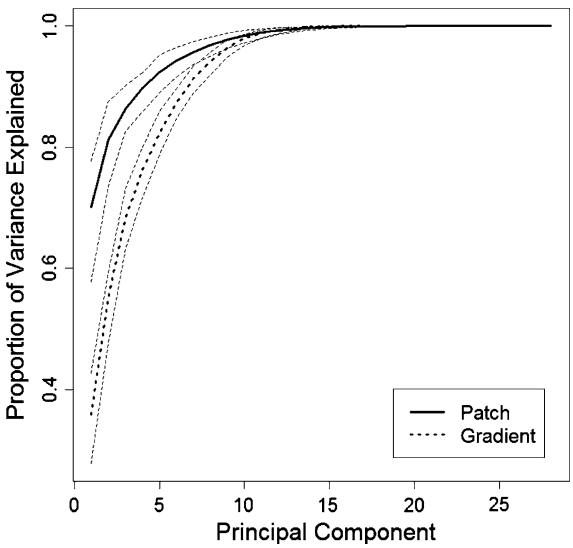

Fig. 2 Scree plot of principal components analysis of 28 patch metrics (Table 3) and 17 surface metrics (Appendix—Electronic Supplementary Material) computed for 264 sample landscapes for each of 16 different patch mosaic models (8 mosaics × 2 window sizes) and 18 different landscape gradient models (9 surfaces × 2 window sizes). The scree plot depicts the cumulative proportion of variance explained (*y*-axis) by an increasing number of principal components (*x*-axis) for each set of metrics. The *thick solid and dotted lines* represent the medians and the *thin dashed lines* represent the minimums and maximums across the 16 patch mosaic models and 18 landscape gradient models, respectively

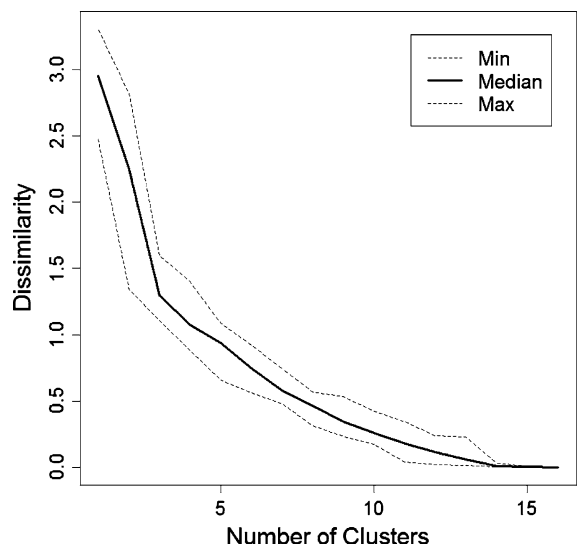

Fig. 3 Scree plot of an agglomerative hierarchical clustering of 17 surface metrics (Appendix—Electronic Supplementary Material) computed for 264 sample landscapes and 18 different landscape gradient models (9 surfaces × 2 window sizes). The scree plot depicts the dissimilarity (*y*-axis) at which surface metrics (and clusters) fuse, read right to left, to form a decreasing number of clusters (*x*-axis). Dissimilarity was based on Spearman rank correlation distance between surface metrics and fusion was based on Ward's minimum-variance method. The *solid line* represents the median and the *dotted lines* represent the minimum and maximum across the 18 landscape gradient models

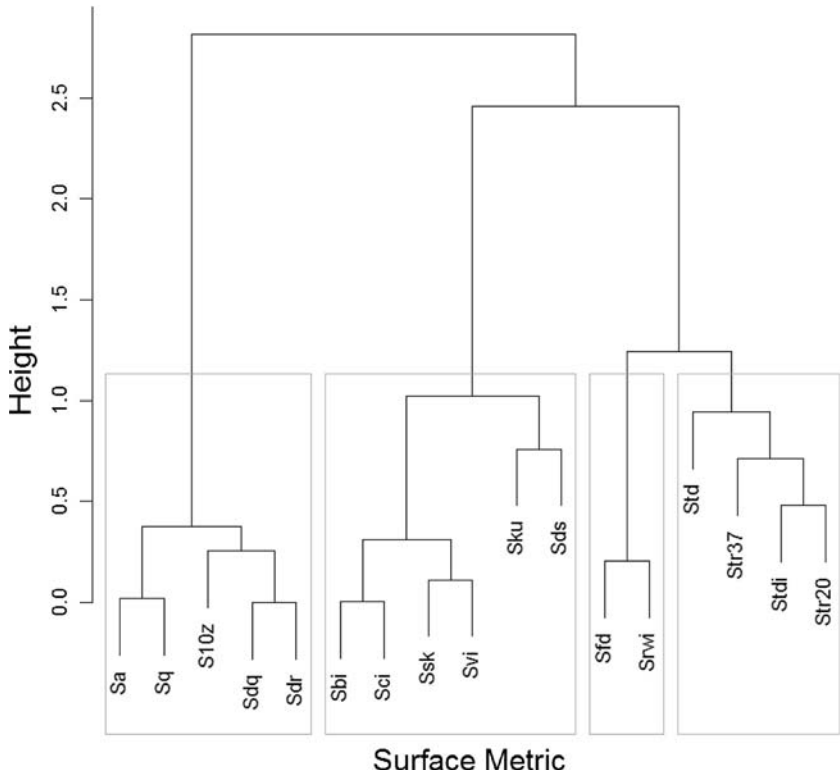

Fig. 4 Dendrogram of an agglomerative hierarchical clustering of 17 surface metrics (Appendix—Electronic Supplementary Material) computed for 264 sample landscapes representing the Tasseled cap greenness index (TsGR) derived from Landsat ETM+ (see Table 2). Clustering was based on Spearman rank correlation distances between surface metrics and Ward's minimum-variance fusion. The leaves of the dendrogram represent individual surface metrics and the hierarchical manner by which they agglomerate into increasingly fewer and larger clusters is given by the height (*y*-axis) at which they are joined together. The *gray boxes* show the four-cluster solution

metrics: *Sa*, *Sq*, *S10z*, *Sdq*, and *Sdr*) and the fourth cluster (comprised of two metrics: *Sfd* and *Srwi*) maintained perfect cohesiveness (cohesiveness index = 1) across landscape models. In other words, all metrics within each of these clusters always clustered together regardless of the landscape model. The second cluster, comprised of five metrics (*Ssk*, *Sku*, *Sbi*, *Sci*, and *Svi)*, maintained the lowest degree of cohesiveness among clusters (cohesiveness index = 0.69). The instability of this cluster was largely due to *Sku*, which "bounced" around somewhat among clusters but more often than not was associated with this cluster. Removing this metric from the cluster increased its cohesiveness to 0.86. The third cluster, comprised of four metrics (*Std*, *Stdi*, *Str20*, and *Str37*), maintained a cohesiveness of 0.74 across models. A single metric, *Sds*, did not consistently cluster with other metrics.

The four clusters of surface metrics varied markedly in their relationships to the patch metrics. The metrics in the first cluster (*Sa*, *Sq*, *S10z*, *Sdq*, and *Sdr*) exhibited strong correlations with a number of patch metrics, although the strength of the individual correlations varied somewhat between the landscape models under comparison. For example, Fig. 6a depicts the average correlations between *Sa* (as a representative of cluster 1) and each of the 28 patch metrics across the three patch mosaic models derived from the DEM (left-hand figure) and across the three patch mosaic models derived from NDVI (right-hand figure). The patch metrics are depicted in rank order from largest positive correlation to largest negative correlation for each of the models. While the exact ordering of patch metrics varies somewhat between the DEM and NDVI models, there is general consistency among the most strongly correlated metrics. In general, the first cluster represents a gradient in overall surface diversity (i.e., vertical variability in the surface), analogous to a gradient in patch richness under the patch model, and spatial heterogeneity and contrast (i.e., horizontal variability in the surface), analogous to a gradient in patchiness and edge contrast under the patch model. Unlike the metrics in the first cluster, the metrics in the remaining three clusters did not exhibit strong and consistent correlations with the patch metrics

	Sa	Sq	S10z	Sdq	Sdr	Ssk	Sku	Sbi	Sci	Svi	Std	Stdi	Str20	Str37	Sfd	Srwi	Sds
Sa	1																
Sq	1	1															
S10z	1	1	1														
Sdq	1	1	1	1													
Sdr	1	1	1	1	1												
Ssk	0	0	0	0	0	1											
Sku	0.167	0.167	0.167	0.167	0.167	0.556	1										
Sbi	0	0	0	0	0	0.778	0.333	1									
Sci	0	0	0	0	0	0.778	0.333	1	1								
Svi	0	0	0	0	0	0.944	0.5	0.833	0.833	1							
Std	0	0	0	0	0	0	0.167	0	0	0	1						
Stdi	0	0	0	0	0	0	0.056	0	0	0	0.778	1					
Str20	0	0	0	0	0	0	0.111	0	0	0	0.556	0.778	1				
Str37	0	0	0	0	0	0	0.111	0	0	0	0.556	0.778	1	1			
Sfd	0.222	0.222	0.222	0.222	0.222	0.056	0.333	0	0	0.056	0.278	0.167	0.222	0.222	1		
Srwi	0.222	0.222	0.222	0.222	0.222	0.056	0.333	0	0	0.056	0.278	0.167	0.222	0.222	1	1	
Sds	0.111	0.111	0.111	0.111	0.111	0.444	0.5	0.333	0.333	0.389	0.389	0.222	0.111	0.111	0.167	0.167	1

Cohesiveness = 1 | Cohesiveness = 0.69 | Cohesiveness = 0.74 | Cohesiveness = 1

Fig. 5 Ordered cluster cohesiveness matrix depicting the proportion of models in which each surface metric co-occurred in the same cluster with each other metric based on a four-cluster solution. Clustering was based on agglomerative hierarchical clustering of 17 surface metrics (Appendix—Electronic Supplementary Material) computed for 264 sample landscapes and 18 different landscape gradient models (9 surfaces × 2 window sizes) using Spearman rank correlation distance between surface metrics and Ward's minimum-variance fusion. The cluster cohesiveness index is the average proportion of co-occurrence among the metrics in each designated cluster. An index of one means the constituent metrics co-occur in the same cluster across all landscape models

(Fig. 6b–d), suggesting that these components of surface structure do not have analogs in patch mosaics, at least based on the patch metrics considered here.

Discussion

Landscape models: from patch mosaics to landscape gradients

One of the preeminent challenges in the study and management of landscapes is characterizing spatial heterogeneity in a manner and at a scale meaningful to the phenomenon under consideration (Li and Wu 2004). Given the nearly ubiquitous use of the patch mosaic model of landscape structure, much of this difficulty is centered on the choice of an appropriate classification of the landscape. In most applications, a single map is created to represent the structure of the landscape and the analysis of pattern–process relationship proceeds with little or no attention to uncertainty in the landscape model—the patch mosaic is taken as correct. One of the critical issues in defining the patch mosaic is selecting an appropriate thematic resolution (i.e., the number of discrete classes to represent). More often than not, the choice of resolution(s) is arbitrary, as only rarely are there ecological data to inform the choice of optimal resolution(s) (Thompson and McGarigal 2002). Moreover, in many applications the final patch mosaic is created by classifying data that is continuous in origin. For example, land cover maps are commonly created by classifying remotely sensed imagery (e.g., Landsat TM/ETM+) and ecological land unit maps are often created by classifying continuous terrain data (e.g., elevation, topographic position, topographic wetness, etc.). In some cases, the classification may be justified by the discrete nature of the spatial heterogeneity (e.g., landscapes with an abundance of human land use practices), but more often than not the classification cannot be justified on grounds other than conventionality and ease of use with existing analytical tools (e.g., FRAGSTATS).

As illustrated in this study, the landscape gradient model offers an alternative to the patch mosaic model when the raw spatial data is continuously scaled. The advent of surface pattern metrics eliminates the necessity of discretely classifying landscapes for the purpose of quantifying landscape patterns, and in so doing eliminates the errors and arbitrariness of the classification process. Given the increasing availability of remotely sensed data, there are almost an

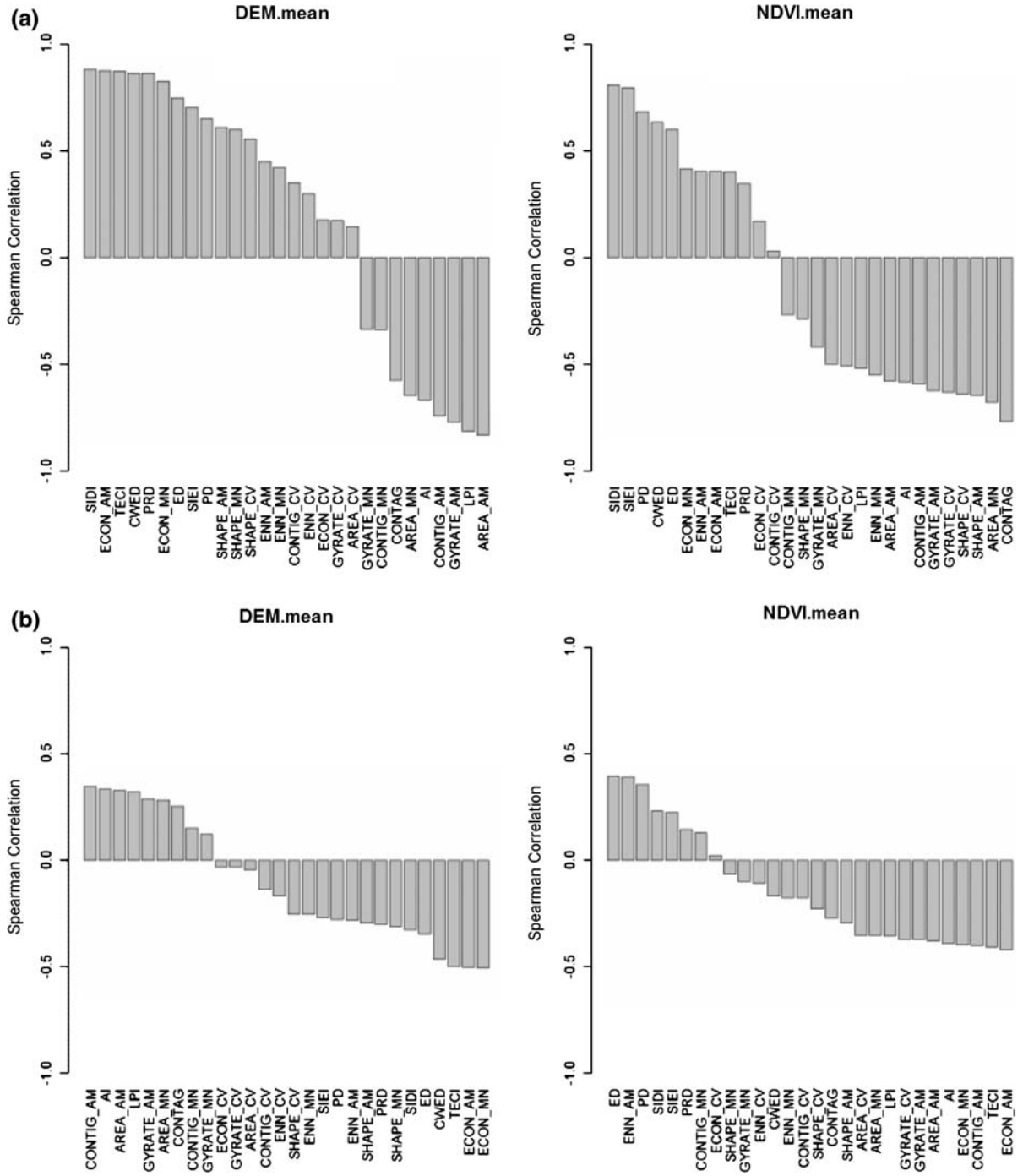

Fig. 6 Histogram of the average pairwise Spearman rank correlations (in rank order from largest positive correlation to largest negative correlation) between **a** surface roughness, **b** surface skewness, **c** dominant texture direction, and **d** radial wavelength index (Appendix—Electronic Supplementary Material) and each of the 28 patch metrics (Table 3) for two different landscape model comparisons. The DEM. mean represents the average correlation between the corresponding surface metric derived from the DEM surface (Table 2) and each patch metric across three patch mosaics derived from the DEM (5, 10, and 15 elevation classes), and similarly for NDVI

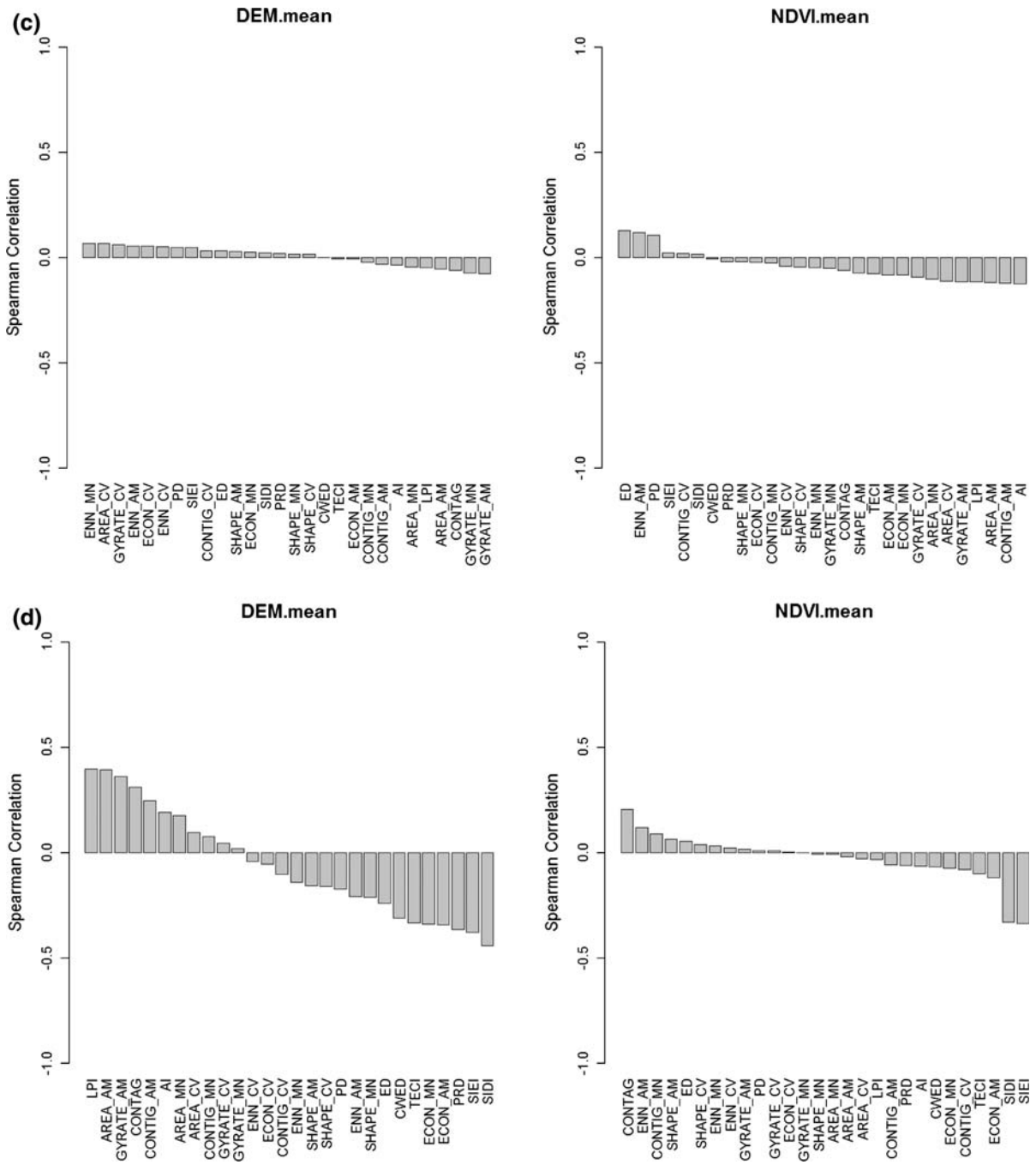

Fig. 6 continued

unlimited number of ways to represent landscape gradients, making it easy to construct alternative landscape gradient models and incorporate model uncertainty into analyses. To demonstrate this flexibility, in this study we constructed nine different landscape gradient models based on Landsat ETM+ and digital elevation data. Each of these models represented an alternative perspective on the underlying spatial heterogeneity of the landscape. Because there was little work involved in preparing these

surfaces and virtually no subjectivity, they allowed us to readily examine uncertainty in our representation of the landscape—in this case, uncertainty in the redundancy and behavior of various surface metrics.

Attributes of surface patterns

Based on our examination of 17 surface metrics applied to 18 landscape gradient models (9 gradient surfaces × 2 window sizes), a number of characteristics of surface patterns stand out. First, like patch mosaics, landscape gradients have both nonspatial and spatial components. The nonspatial components refer solely to the vertical variability in the surface, whereas the spatial components refer to the horizontal (and vertical) variability in the surface. More specifically, the nonspatial components refer to variability in the overall height distribution of the surface, but not the spatial arrangement, location or distribution of surface peaks and valleys. As such, the nonspatial surface metrics (Appendix—Electronic Supplementary Material) measure aspects of landscape composition, not configuration, and are akin to measures of patch type diversity in the patch mosaic paradigm. Conversely, the spatial components refer to the arrangement, location or distribution of surface peaks and valleys. As such, the spatial surface metrics (Appendix—Electronic Supplementary Material) measure aspects of landscape configuration.

Second, in contrast to the suite of available patch metrics, the available surface metrics (including those investigated here) are all "structural" metrics. Structural metrics measure physical properties of the landscape pattern independent of the process under investigation, and thus do not require any additional user parameterization (McGarigal 2002). In contrast, many of the patch metrics are functional (e.g., edge contrast and core area), requiring user parameterization that renders them functionally related to the process under consideration (McGarigal 2002). While this difference is noteworthy, it may simply be a reflection of the early stage of development of surface metrics intended for ecological application.

Third, as with patch mosaics, there are several structural components of landscape gradients. We observed four relatively distinct components of landscape structure based on empirical relationships among the 17 surface metrics across the 18 landscape gradient models.

Surface roughness

The dominant structural component of the surfaces we examined was actually a combination of two distinct sub-components: (1) the overall variability in surface height and (2) the local variability in slope. The first sub-component refers to the nonspatial (composition) aspect of the vertical height profile; that is, the overall variation in the height of the surface without reference to the horizontal variability in the surface, and is represented by three surface amplitude metrics: average roughness (*Sa*), root mean square roughness (*Sq*), and ten-point height (*S10z*) (Appendix—Electronic Supplementary Material). These metrics are analogous to the patch type diversity measures (e.g., Simpson's diversity index) in the patch mosaic paradigm, whereby greater variation in surface height equates to greater landscape diversity. Importantly, while these metrics reflect overall variability in surface height, they say nothing about the spatial heterogeneity in the surface.

The second sub-component refers to the spatial (configuration) aspect of surface roughness with respect to local variability in height (or steepness of slope), and includes two surface metrics: surface area ratio (*Sdr*) and root mean square slope (*Sdq*) (Appendix—Electronic Supplementary Material). These metrics are analogous to the edge density and contrast metrics (e.g., contrast-weighted edge density, total edge contrast index) in the patch mosaic paradigm, whereby greater local slope variation equates to greater density and contrast of edges. Interestingly, while these surface metrics reflect something akin to edge contrast, they do so without the need to supply edge contrast weights because they are structural metrics. These two metrics appear to have the greatest overall analogy to the patch-based measures of spatial heterogeneity and overall patchiness. A fine-grained patch mosaic (as represented by any number of common patch metrics, such as mean patch size or density) is conceptually equivalent to a rough surface with high local variability.

On conceptual and theoretical grounds, these spatial and nonspatial aspects of surface roughness are independent components of landscape structure; however, in the landscape gradients we examined these two aspects were highly correlated empirically. This distinction between conceptually and/or theoretically related metrics and groupings based on their

empirical behavior has also been demonstrated for patch metrics (Neel et al. 2004).

Shape of the surface height distribution

Another important nonspatial (composition) component of the surfaces we examined was the shape of the surface height distribution. This component was comprised of five metrics: skewness (*Ssk*), kurtosis (*Sku*), surface bearing index (*Sbi*), valley fluid retention index (*Svi*), and core fluid retention index (*Sci*). All of these metrics measure departure from a Gaussian distribution of surface heights, but emphasize different aspects of departure from normality (Appendix—Electronic Supplementary Material). *Ssk* and *Sku* measure the familiar skewness and kurtosis of the surface height distribution, while the surface bearing metrics, *Sbi*, *Sci*, and *Svi*, measure different aspects of the surface height distribution in its cumulative form (Fig. 7). This component was universally present across landscape models, but the composition of metrics varied somewhat among models reflecting the complexities inherent in measuring non-parametric shape distributions. There were no strong patch mosaic analogs to these surface metrics (Fig. 6b); however, departure from a Gaussian distribution of surface heights was weakly correlated with, and conceptually most closely related to, patch-based measures of landscape dominance (or its compliment, evenness) such as Simpson's evenness index (*SIEI*) and largest patch index (*LPI*). Importantly, these five surface metrics measure the 'shape' of the surface height distribution and are not affected by the surface roughness (as defined earlier) per se.

Angular texture

A third prominent component of the surfaces we examined was the angular orientation (direction) of the surface texture and its magnitude. This

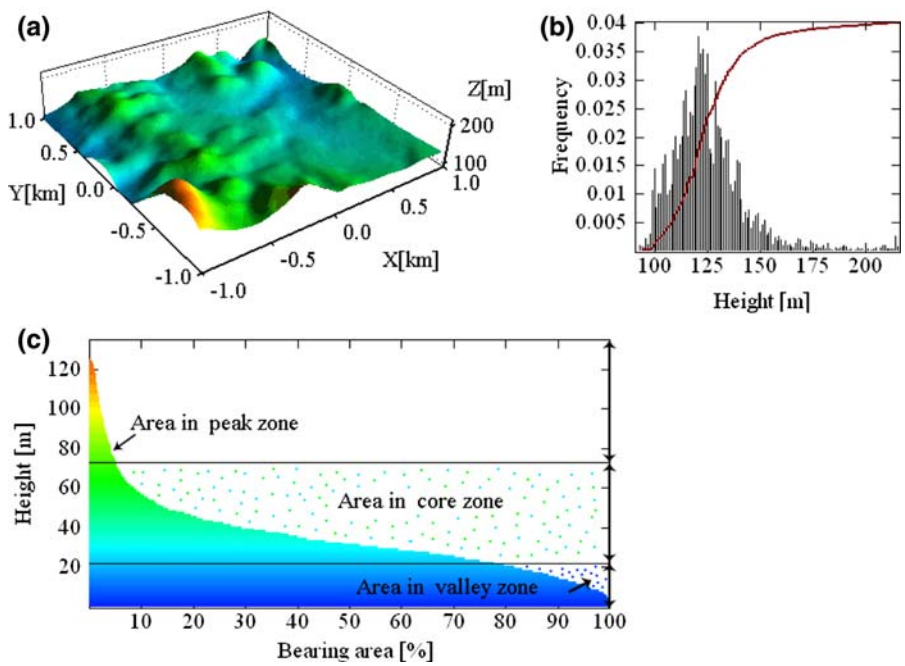

Fig. 7 Surface bearing area curve (also called the Abbott curve) representing the cumulative form of the surface height distribution. **a** An arbitrarily selected landscape represented with the DEM landscape gradient model. **b** The surface height distribution shown as a frequency distribution (*bars*) and as a cumulative frequency (*line*). **c** The surface bearing area curve is the inverted cumulative height distribution; it is divided into zones to highlight different parts of the height profile. Generally, the "peak" zone corresponds to the top 5% of the surface height range, the "core" zone corresponds to the 5–80% height range, and the "valley" zone corresponds to the bottom 20% of the height range. The void volume (area above the bearing area curve) in the 'core' zone (shown in light stippling) is used in the core fluid retention index (*Sci*). Similarly, the void volume in the 'valley' zone (shown in dark stippling) is used in the valley fluid retention index (*Svi*)

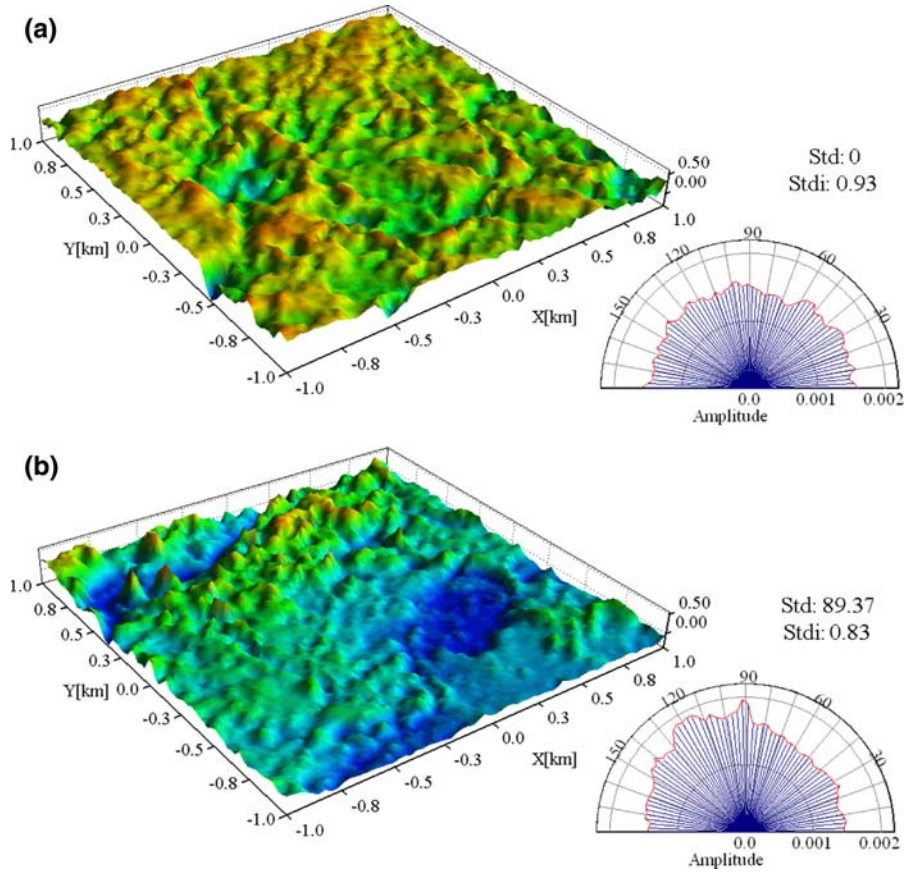

Fig. 8 Angular texture can be calculated from the Fourier spectrum (see Appendix—Electronic Supplementary Material). The angular spectrum (shown below and to the right of each image) depicts the relative amplitudes for M equally spaced angles. A larger amplitude in one direction indicates a dominant lay or orientation in the surface. The sample landscapes shown here based on the NDVI landscape gradient model illustrate the differences in angular texture we observed: **a** no texture orientation (*Std* = 0; *Stdi* = 0.93); **b** mild texture orientation (*Stdi* = 0.83) at approximately 89° (*Std* = 89.37)

component is inherently spatial, since the arrangement of surface peaks and valleys determines whether the surface has a particular orientation or not, and is represented by four spatial metrics: dominant texture direction (*Std*), texture direction index (*Stdi*), and two texture aspect ratios (*Str20* and *Str37*). The computational methods behind these metrics are too complex to describe here (but see Appendix—Electronic Supplementary Material), but are based on common geostatistical methods (Fourier spectral analysis and autocorrelation functions) that determine the degree of anisotropy (orientation) in the surface. Not surprisingly given our knowledge of the study landscape, we did not observe sample landscapes with a strong texture orientation. We did observe mild levels of texture orientation in some landscapes, but many were without apparent orientation (Fig. 8). Importantly, the measurement of texture direction has no obvious analog in the patch mosaic paradigm; indeed, we observed no pairwise correlation greater than $\pm$ 0.22 between any of these four surface metrics and any of the 28 patch metrics (Fig. 6c).

Radial texture

The fourth prominent component of the surfaces we examined was the radial texture of the surface and its magnitude. Radial texture refers to repeated patterns of variation in surface height radiating outward in concentric circles from any location. Like angular texture, this component is inherently spatial, since the arrangement of surface peaks and valleys determines whether the surface has any radial texture or not, and is represent by three spatial metrics: dominant radial wavelength (*Srw*), radial wave index (*Srwi*), and fractal dimension (*Sfd*). Again, the computational methods behind these metrics are based on common geostatistical methods (see Appendix—Electronic Supplementary Material). A limitation of these and other metrics based on Fourier spectral analysis and

autocorrelation functions is that they are only sensitive to repeated, regular patterns. We observed that in the absence of a prominent radial texture, the dominant radial wavelength (*Srw*) ends up being equal to the diameter of the sample landscape. As a result, in some of our landscape gradient models we observed too little variation in this metric and were forced to drop it from the final analyses. Despite these limitations, we observed sample landscapes with varying degrees of radial texture based on the other two metrics (Fig. 9). In contrast to angular texture, the measurement of radial texture has at least one conceptual analog in the patch mosaic paradigm—mean and variability in nearest neighbor distance. On conceptual grounds, *Srw* should equate to mean nearest neighbor distance, and *Srwi* and *Sfd* should equate to the coefficient of variation in nearest neighbor distance. However, in our study the corresponding pairwise correlations did not exceed ± 0.22, nor were there any pairwise correlations greater than ± 0.40 between either of these surface metrics and any of the 28 patch metrics (Fig. 6d).

Conclusions

The quantification of landscape structure is generally considered prerequisite to the study of pattern–process relationships. In this paper, we described a variety of surface metrics that allow for the quantification of landscape gradients, paving the way for an expanded landscape ecology that encompasses continuous as well as categorical representations of spatial heterogeneity. Among other findings, we demonstrated that landscape gradient surfaces are multivariate, similar to patch mosaics, and thus cannot be characterized by any single metric. We

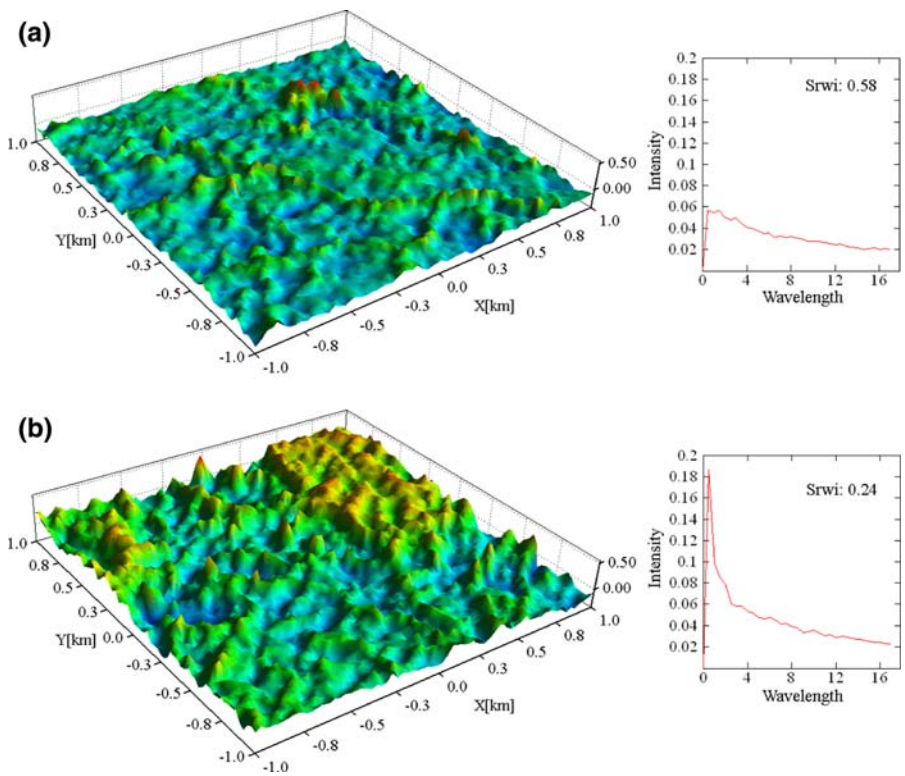

Fig. 9 Radial texture can be calculated from the Fourier spectrum (see Appendix—Electronic Supplementary Material). The radial spectrum (shown to the right of each image) depicts the relative amplitudes (intensity) for M/(2–1) equidistantly separated semicircles. A larger amplitude at one distance (wavelength) indicates a dominant radial pattern in the surface. The sample landscapes shown here based on the NDVI landscape gradient model illustrate the differences in radial texture we observed: **a** weak radial texture (*Srwi* = 0.58); **b** strong radial texture (*Srwi* = 0.24). Both sample landscapes have a dominant radial texture at very short wavelengths (i.e., distances) indicating a relatively fine-scale to the peaks and valleys

identified four distinct structural components that were universally present across 18 different landscape gradient models and suggest these represent a minimum set of structural components for landscape gradients. In addition, we demonstrated that landscape gradients have properties that do not have obvious analogs in patch mosaics. Thus, the landscape gradient model has the potential to reveal unique insights into pattern–process relationships.

While our study demonstrates the feasibility of quantifying the structure of landscape gradients using surface metrics well known in the field of surface metrology, several critical challenges remain. While we examined the behavior of surface metrics computed at two window sizes (i.e., landscape extents), a thorough examination of the scaling behavior of these metrics (across both grain and extent, as in Wu et al. 2002) remains a priority for future research. Most importantly, it remains to be widely demonstrated that surface metrics can be useful in ecological applications relating landscape pattern to process. It is insufficient to be able to quantify surface patterns; the measured surface patterns must be shown to have a clear relationship with ecological process for the metrics to be deemed useful (Li and Wu 2004). However, the stage is set for landscape ecologists to critically evaluate the gradient model and surface metrics for their utility in studying and managing heterogeneous landscapes. One recent application used 11 surface metrics derived from a DEM as predictor variables in tree occurrence models (Evans and Cushman submitted). A practical obstacle to meeting this challenge is the lack of accessible software. While several software packages exist for quantifying surface patterns (SPIP™, TrueMap™, MountainsMap™, GLCMSurf™, and Omnisurf™; see reference Gadelmawla (2004), most are expensive, difficult to use and poorly documented. Consequently, it remains a priority to implement these methods in tools such as FRAGSTATS that are readily available and familiar to landscape ecologists. Otherwise, the computational demands of surface metrics are generally comparable to those of patch metrics.

Acknowledgments We thank Brad Compton and Brad Timm for comments on a draft of this manuscript. This material is based on work partially supported by the Cooperative State Research, Extension, Education Service, US Department of Agriculture, Massachusetts Agricultural Experiment Station and the Department of Natural Resources Conservation, under Project No. 3321, and The Scientific and Technological Research Council of Turkey, under project International Postdoctoral Research Scholarship Programme-2219.

References

Austin MP (1999a) The potential contribution of vegetation ecology to biodiversity research. Ecography 22:465–484. doi:10.1111/j.1600-0587.1999.tb01276.x

Austin MP (1999b) A silent clash of paradigms: some inconsistencies in community ecology. Oikos 86:170–178. doi:10.2307/3546582

Austin MP, Smith TM (1989) A new model for the continuum concept. Vegetatio 83:35–47. doi:10.1007/BF00031679

Barbato G, Carneiro K, Cuppini D, Garnaes J, Gori G, Hughes G, Jensen CP, Jorgensen JF, Jusko O, Livi S, McQuoid H, Nielsen L, Picotto GB, Wilening G (1995) Scanning tunnelling microscopy methods for the characterization of roughness and micro hardness measurements. Synthesis report for research contract with the European Union under its programme for applied metrology. European Commission Catalogue number: CD-NA-16145 EN-C Brussels Luxemburg

Beasom SL (1983) A technique for assessing land surface ruggedness. J Wildl Manage 47:1163–1166. doi:10.2307/3808184

Cushman SA, McGarigal K, Neel MC (2008) Parsimony in landscape metrics: strength, universality, and consistency. Ecol Indic 8:691–703. doi:10.1016/j.ecolind.2007.12.002

Dorner B, Lertzman K, Fall J (2002) Landscape pattern in topographically complex landscapes: issues and techniques for analysis. Landscape Ecol 17:729–743. doi:10.1023/A:1022944019665

ERDAS (1999) ERDAS field guide, 5th edn. ERDAS Inc., Atlanta

Fischer J, Lindenmayer DB (2006) Beyond fragmentation: the continuum model for fauna research and conservation in human-modified landscapes. Oikos 112:473–480. doi:10.1111/j.0030-1299.2006.14148.x

Forman RTT (1995) Land mosaics: the ecology of landscapes and regions. Cambridge University Press, Cambridge

Forman RTT, Godron M (1986) Landscape Ecol. Wiley, New York

Gadelmawla ES (2004) A vision system for surface roughness characterization using the gray level co-occurrence matrix. NDT&E Int 37:577–588. doi:10.1016/j.ndteint.2004.03.004

Gadelmawla ES, Koura MM, Maksoud TMA, Elewa IM, Soliman HH (2002) Roughness parameters. J Mater Process Technol 123:133–145. doi:10.1016/S0924-0136(02)00060-2

Hoechstetter S, Walz U, Dang LH, Thinh NX (2008) Effects of topography and surface roughness in analyses of landscape structure—a proposal to modify the existing set of landscape metrics. Landsc Online 1:1–14

Jenness J (2004) Calculating landscape surface area from digital elevation models. Wildl Soc Bull 32:829–839. doi:10.2193/0091-7648(2004)032[0829:CLSAFD]2.0.CO;2

Jenness J (2005) Topographic position index (tip_jen.avx) extension for ArcView 3.x., Jenness Enterprises. Available from http://www.jennessent.com/arview/tpi.htm

Li H, Wu J (2004) Use and misuse of landscape indices. Landscape Ecol 19:389–399. doi:10.1023/B:LAND.0000030441.15628.d6

Manning AD, Lindenmayer DB, Nix HA (2004) Continua and Umwelt: novel perspectives on viewing landscapes. Oikos 104:621–628. doi:10.1111/j.0030-1299.2004.12813.x

McCune B, Keon D (2002) Equations for potential annual direct incident radiation and heat load. J Veg Sci 13:603–606. doi:10.1658/1100-9233(2002)013[0603:EFPADI]2.0.CO;2

McGarigal K (2002) Landscape pattern metrics. In: El-Shaarawi AH, Piegorsch WW (eds) Encyclopedia of environmetrics, vol 2. Wiley, Chichester, pp 1135–1142

McGarigal K, Cushman SA (2005) The gradient concept of landscape structure. In: Wiens J, Moss M (eds) Issues and perspectives in landscape ecology. Cambridge University Press, Cambridge, pp 112–119

McGarigal K, Cushman SA, Stafford SG (2000) Multivariate statistics for wildlife and ecology research. Springer, New York

McGarigal K, Cushman SA, Neel MC, Ene E (2002) FRAGSTATS: spatial pattern analysis program for categorical maps. Computer software program produced by the authors at the University of Massachusetts, Amherst. Available from http://www.umass.edu/landeco/research/fragstats/fragstats.html

McIntyre S, Barrett GW (1992) Habitat variegation, an alternative to fragmentation. Conserv Biol 6:146–147. doi:10.1046/j.1523-1739.1992.610146.x

Melton MA (1957) An analysis of the relations among elements of climate, surface properties, and geomorphology. Columbia University, Department of Geology, Project NR 389–042, Tech. Rep. 11, New York, 102 pp

Moore ID, Gryson RB, Ladson AR (1991) Digital terrain modeling: a review of hydrological, geomorphological, and biological applications. Hydrol Process 5:3–30. doi:10.1002/hyp.3360050103

Moore ID, Gessler PE, Nielsen GA, Petersen GA (1993) Terrain attributes: estimation methods and scale effects. In: Jakeman AJ, Beck MB, McAleer M (eds) Modeling change in environmental systems. Wiley, London, pp 189–214

MountainsMap™ Surface analysis software based upon mountains technology, Digital Surf. Available from http://www.digitalsurf.fr/en/index.html

NanoRule+™ AFM image analysis software, Pacific Nanotechnology, Inc.. Available from http://www.pacificnano.com/analysis-software.html

Neel MC, McGarigal K, Cushman SA (2004) Behavior of class-level landscape metrics across gradients of class aggregation and area. Landscape Ecol 19:435–455. doi:10.1023/B:LAND.0000030521.19856.cb

OmniSurf™ Image analysis software, Digital Metrology Solutions, Inc.. Available from http://www.digitalmetrology.com/

Parker KC, Bendix J (1996) Landscape-scale geomorphic influences on vegetation patterns in four environments. Phys Geogr 17:113–141

Pike RJ (2000) Geomorphometry—diversity in quantitative surface analysis. Prog Phys Geogr 24:1–20

R Development Core Team (2008) R: A language and environment for statistical computing. R Foundation for Statistical Computing, Vienna. ISBN 3-900051-08-9. Available from http://www.R-project.org

Ramasawmy H, Stout KJ, Blunt L (2000) Effect of secondary processing on EDM surfaces. Surf Eng J 16:501–505

Sanson GD, Stolk R, Downes BJ (1995) A new method for characterizing surface roughness and available space in biological systems. Functional Ecol 9:127–135

Schumm SA (1956) Evolution of drainage basins and slopes in badlands at Perth Amboy, New Jersey. Bull Geol Soc Am 67:597–646

SPIP™ The scanning probe image processor. Image metrology APS, Lyngby. Available from http://www.imagemet.com/

Stout KJ, Sullivan PJ, Dong WP, Mainsah E, Lou N, Mathia T, Zahouani H (1994) The development of methods for the characterization of roughness on three dimensions. Publication no EUR 15178 EN of the Commission of the European Communities, Luxembourg

Strahler AN (1952) Hypsometric (area-altitude) analysis of erosional topography. Bull Geol Soc Am 63:1117–1142

Thompson CM, McGarigal K (2002) The influence of research scale on bald eagle habitat selection along the lower Hudson River, New York. Landscape Ecol 17:569–586

TrueMap™ Surface topography visualization and analysis software. TrueGage™ surface metrology. Available from http://www.truegage.com/

Tucker CJ (1979) Red and photographic infrared linear combinations for monitoring vegetation. Remote Sensing of the Environment 8:127–150

Turner MG (2005) Landscape ecology: what is the state of the science? Annu Rev Ecol Evol Syst 36:319–344

Turner MG, Gardner RH, O'Neill RV (2001) Landscape ecology in theory and practice. Springer, New York

Villarrubia JS (1997) Algorithms for scanned probe microscope, image simulation, surface reconstruction and tip estimation. J Nat Inst Stand and Technol 102:435–454

Wiens JA (1989) Spatial scaling in ecology. Functional Ecol 3:385–397

Wilson JP, Gallant JC (2000) Terrain analysis: principles and applications. Wiley, New York

Wu JG, Shen W, Sun W, Tueller PT (2002) Empirical patterns of the effects of changing scale on landscape metrics. Landscape Ecol 17:761–782

Appendix. Brief description of some common surface metrics applied in this study. Metrics are grouped into "families" based on the surface properties measured; names, acronyms and descriptions follow that given in the SPIP software program (SPIP). See the program documentation for formulas. See SPIP documentation and Gadelmawla et al (2002) for additional surface metrics. Note, all of these metrics can be calculated with or without correcting for the overall mean height of the surface or a plane (of any order) fit to the surface. In the descriptions, where it matters we define and interpret these metrics based on a correction for the overall mean.

Metric Name	Description
Amplitude Metrics: measure vertical characteristics of the surface deviations. These metrics are sensitive to variability in the overall height distribution, but not the spatial arrangement, location or distribution of surface peaks and valleys. As such, these parameters measure aspects of landscape composition, not configuration.	

Average roughness (*Sa*)	The average absolute deviation of the surface heights from the mean. This is a general measure of overall surface variability and can be interpreted as a nonspatial measure of landscape diversity, analogous to the patch-based diversity metrics. Larger values represent an increasing range of values in the surface attribute (akin to increasing patch richness) and/or an increasing spread in the distribution of area among levels (heights) of the surface attribute (akin to increasing patch evenness). Importantly, this metric does not differentiate among different shapes of the surface height profile.
Root mean-square roughness (*Sq*)	The standard deviation of the distribution of surface heights. This is a general measure of overall surface variability like *Sa*, but it is more sensitive than *Sa* to large deviations from the surface mean. Otherwise, this metric has the same general interpretation as *Sa* and is likely to be highly correlated with *Sa* in real-world applications.
Ten-point height (*S10z*)	Average height above the mean height of the surface of the five highest local maximums plus the average height below the mean height of the surface of the five lowest local minimums. This is a general measure of overall surface variability like *Sa* and *Sq*, but it is particularly sensitive to occasional high peaks or deep valleys. Otherwise, this metric has the same general interpretation as *Sa* and *Sq* and is likely to be correlated with them in real-world applications.

Surface skewness (*Ssk*)	Asymmetry of the surface height distribution. This is a measure of the symmetry of the surface height profile about the mean. It is sensitive to occasional deep valleys or high peaks. A surface with as many peaks as valleys has zero skewness. Profiles with peaks removed or occasional deep valleys have negative skewness; profiles with valleys filled in or occasional high peaks have positive skewness. Consequently, the value of skewness depends on whether the bulk of the surface is above (negative skewed) or below (positive skewed) the mean surface height. High skewness, either positive or negative, indicates a landscape with a dominant surface height, akin to having a 'matrix' under the patch mosaic model of landscape structure. Thus, this metric can be interpreted as a measure of landscape dominance (or its complement, evenness), akin to the patch-based evenness metrics.

Surface kurtosis (*Sku*)	Peaked-ness of the surface distribution. Like *Ssk*, this is a measure of the shape of the surface height profile about the mean line and is likewise sensitive to occasional deep valleys or high peaks. A surface with a relatively even distribution of heights above and below the mean has low kurtosis and is said to by platykurtic (*Sku* < 3). A surface with relatively little area high above or below the mean has high kurtosis and is said to be leptokurtic (*Sku* > 3). Consequently, high kurtosis indicates a landscape with a dominant surface height, akin to a 'matrix' under the patch mosaic model of landscape structure; whereas, low kurtosis indicates a landscape with an even distribution among surface heights. Thus, like *Ssk*, this metric can be interpreted as a measure of landscape dominance (or its complement, evenness). Interpreted in combination, surface skewness and kurtosis indicate the degree of landscape dominance and the nature of that dominance.

Surface Bearing Metrics: measure vertical characteristics of the surface deviations like the amplitude metrics above, but these metrics are based on the surface bearing area ratio curve (also called the Abbott curve) computed by inversion of the cumulative height distribution histogram (Fig. 7). The bearing area curve represents the cumulative form of the surface height distribution used in the amplitude metrics. Generally, the bearing area curve is divided into three zones, called the "peak" zone, corresponding to the top 5% of the surface height range, "core" zone, corresponding to the 5% - 80% height range, and "valley" zone, which corresponds to the bottom 20% of the height range of the surface. Like the amplitude metrics, these metrics are sensitive to variability in the overall height distribution, but not the spatial arrangement, location or distribution of surface peaks and valleys. As such, these parameters likewise measure aspects of landscape composition, not configuration.

Surface bearing index (*Sbi*)	Ratio of the root mean square roughness (*Sq*) to the height from the top of the surface to the height at 5% bearing area (Fig. 7). Like *Ssk* and *Sku*, this too is a measure of the shape of the surface height profile. However, *Sbi* is particularly sensitive to occasional high peaks and not occasional deep valleys. For a Gaussian height distribution *Sbi* approaches 0.608. A surface with relatively few high peaks has a low surface bearing index (*Sbi* < 0.608). A surface with relatively many high peaks or without high peaks at all has a high surface bearing index (*Sbi* > 0.608). Consequently, like *Ssk* and *Sku*, this metric can be interpreted as a measure of landscape dominance (or its complement, evenness), but with additional information as to the nature of the surface composition.

Valley fluid retention index (*Svi*)	Void volume (area above the Abbott curve) in the 'valley' zone (Fig. 7). Like *Ssk* and *Sku*, this too is a measure of the shape of the surface height profile. In contrast to *Sbi*, *Svi* is particularly sensitive to occasional deep valleys and not occasional high peaks. For a Gaussian height distribution *Svi* approaches 0.11. A surface with relatively few deep valleys has a low valley fluid retention index (*Svi* < 0.11). A surface with relatively many deep valleys has a high valley fluid retention index (*Svi* > 0.11). Consequently, like *Ssk* and *Sku*, this metric can be interpreted as a measure of landscape dominance (or its complement, evenness), but with additional information as to the nature of the surface composition.

Core fluid retention index (*Sci*)	Void volume (area above the bearing area curve) in the 'core' zone (Fig. 7). Like *Ssk* and *Sku*, this too is a measure of the shape of the surface height profile. In contrast to *Sbi* and *Svi*, *Sci* is sensitive to both occasional high peaks and occasional deep valleys. For a Gaussian height distribution *Sci* approaches 1.56. A surface with relatively few high peaks and/or low valleys has a high core fluid retention index (Sci > 1.56). A surface with relatively many high peaks and/or low valleys has a low core fluid retention index (Sci < 1.56). Consequently, like *Ssk, Sk*u and the other surface bearing metrics, this metric can be interpreted as a measure of landscape dominance (or its complement, evenness), but with additional information as to the nature of the surface composition.

Spatial Metrics: measure combined horizontal and vertical characteristics of the surface deviations. These metrics describe the density of summits, orientation (direction) of the surface texture (based on the Fourier spectrum), and slope gradients of the local surface. These metrics are sensitive to variability in the overall height distribution as well as the spatial arrangement, location or distribution of surface peaks and valleys. As such, these parameters measure aspects of landscape configuration.

Summit density (*Sds*)	Number of local peaks per area. This is a simple measure of overall spatial variability in surface height and is analogous to patch density in the world of patch metrics. Larger values represent increasing spatial heterogeneity in the surface attribute, but the parameter is sensitive to noisy peaks so it should be interpreted carefully.
Surface area ratio (*Sdr*)	Ratio between the surface area to the area of the flat plane with the same x-y dimensions. For a totally flat surface, the surface area and the area of the xy plane are the same and *Sdr* = 0 %. *Sdr* increases as the local slope variability increases. This metric is somewhat analogous to the contrast-weighted edge density metric in the world of patch metrics, because increasing variability and steepness of local slopes is analogous to increasing density of edges and the magnitude contrast between abutting patches along those edges.
Root mean square slope (*Sdq*)	Variance in the local slope across the surface. This is a general measure of surface contrast like *Sdr*, but it is more sensitive than *Sdr* to very steep slopes (i.e., abrupt edge-like changes in surface height). Otherwise, this metric has the same general interpretation as *Sdr* and is likely to be highly correlated with *Sdr* in real-world applications.

Dominant texture direction (*Std*)	Angle of the dominating texture in the image calculated from the Fourier spectrum. The relative amplitudes for the different angles are found by summation of the amplitudes along M equiangularly separated radial lines, as shown in figure 8. The result is called the *angular spectrum*. *Std* is scaled to give the angle with the maximum amplitude sum and ranges between 0-180. Note, this parameter is only meaningful if there is a dominating direction on the sample, and is given as 0 for areas without a dominant texture direction (e.g., flat areas). Importantly, this parameter has no analog in the world of patch metrics.
Texture direction index (*Stdi*)	Relative dominance of *Std* over other directions of texture, defined as the average amplitude sum over all directions divided by the amplitude sum of the dominating direction. *Stdi* ranges from 0 to 1. Surfaces with very dominant directions will have *Stdi* values close to zero and if the amplitude sum of all directions are similar, *Stdi* is close to 1. Like *Std*, this metric has no analog in the world of patch metrics.

Dominant radial wavelength (*Srw*)[1]	Dominating wavelength found in the radial Fourier spectrum. The radial spectrum is calculated by summation of amplitude values around M/(2 -1) equidistantly separated semicircles as indicated in figure 9. The result is called the *radial spectrum*. *Srw* gives the radial distance with the maximum amplitude sum. Because this metric is based on the Fourier spectrum, it is only sensitive to regular patterns of radial variation in surface heights. In practice, in the absence of regular radial patterns, this metric returns a wavelength equal to the diameter of the landscape. Importantly, this parameter has no direct analog in the world of patch metrics, although it is conceptually akin to the mean distance between patches (i.e., mean nearest neighbor distance) when the spacing between patches is somewhat uniform; that is, when the coefficient of variation in nearest neighbor distances is very small.

Radial wavelength index (*Srwi*)	Relative dominance of *Srw* over other radial distances, defined as the average amplitude sum over all radial distances divided by the amplitude sum of the dominating wavelength. *Srwi* ranges from 0 to 1. Surfaces with very dominant radial wavelengths will have *Srdi* values close to zero and if there is no dominating wavelength, *Srwi* is close to 1. Like *Srw*, this metric has no direct analog in the world of patch metrics, although it is conceptually related to the coefficient of variation in nearest neighbor distance since smaller values imply increasing regularity in the spacing of surface height deviations.

Texture aspect ratio (*Str20* & *Str37*)	Defined as the ratio of the fastest to slowest decay to correlation 20% and 37% (by convention) of the autocorrelation function, respectively. Briefly, the autocorrelation of a surface is a surface itself, indicating the spatial autocorrelation in all directions. The autocorrelation surface always includes a central peak with a standard amplitude of 1. The form of the central peak is an indicator of the isotropy of the surface. *Str* is calculated by thresholding the central peak at a specified level, e.g., 0.2 and 0.37. The minimum and maximum radii are sought on the image of the central lobe remaining after thresholding. If the surface presents the same characteristics in every direction the central lobe will be approximately circular and the min and max radii will be approximately equal. If the surface presents a strong orientation, the central lobe will be stretched out and the max radius will be much greater than the min radius. Thus, *Str* ranges from 0 to 1. For a surface with a dominant lay, *Str* will tend towards zero, whereas a spatially isotropic texture will result in a *Str* value of 1. This metric has no direct analog in the world of patch metrics.

Fractal dimension (*Sfd*)	Calculated for the different angles of the angular spectrum by analyzing the Fourier amplitude spectrum (see *Std*); for different angles the Fourier profile is extracted and the logarithm of the frequency and amplitude coordinates calculated. The fractal dimension for each direction is then calculated as 2.0 minus the slope of the log - log curves. *Sfd* ranges from 2 to 4; larger values indicate a fractal surface with an increasing dominant radial wavelength.

[1] *Srw* is included in the table for completeness, but it was not included in the analyses reported in this paper.